

# Type Ia Supernovae are Good Standard Candles in the Near Infrared: Evidence from PAIRITEL

W. Michael Wood-Vasey<sup>1</sup>, Andrew S. Friedman<sup>1</sup>, Joshua S. Bloom<sup>2,3</sup>, Malcolm Hicken<sup>1</sup>, Maryam Modjaz<sup>2</sup>, Robert P. Kirshner<sup>1</sup>, Dan L. Starr<sup>2</sup>, Cullen H. Blake<sup>1</sup>, Emilio E. Falco<sup>1</sup>, Andrew H. Szentgyorgyi<sup>1</sup>, Peter Challis<sup>1</sup>, Stéphane Blondin<sup>1</sup>, and Armin Rest<sup>4,5</sup>

wmwood-vasey@cfa.harvard.edu, afriedman@cfa.harvard.edu,  
 j bloom@astro.berkeley.edu, mhicken@cfa.harvard.edu,  
 mmodjaz@astro.berkeley.edu, rkirshner@cfa.harvard.edu,  
 dstarr@astro.berkeley.edu, cblake@cfa.harvard.edu, efalco@cfa.harvard.edu,  
 saint@cfa0.cfa.harvard.edu, pchallis@cfa.harvard.edu,  
 sblondin@cfa.harvard.edu, arest@physics.harvard.edu

February 6, 2020

## ABSTRACT

We have obtained 1065 near-infrared (NIR;  $JHK_s$ ) measurements of 19 Type Ia supernovae (SNe Ia) using PAIRITEL, the 1.3-m Peters Automated InfraRed Imaging TElescope at Mount Hopkins, Arizona. This new set of observations doubles the number of well-sampled NIR SN Ia light curves. These data strengthen the evidence that SNe Ia are excellent standard candles in the NIR, even without correction for light-curve shape or for reddening. We construct fiducial NIR templates for normal SNe Ia from our sample, excluding only the two known peculiar SNe Ia, SN 2005hk and SN 2005ke. The  $H$ -band absolute magnitudes in this sample of 17 SNe Ia have an *uncorrected* intrinsic RMS of only 0.14 mag. This variation is as small as the scatter in luminosity distance measurements currently used for cosmology that are based on optical light curves after corrections for light-curve shape and for dust absorption. Combining the homogeneous PAIRITEL measurements with 17 SNe Ia from the literature, these

---

<sup>1</sup>Harvard-Smithsonian Center for Astrophysics, 60 Garden Street, Cambridge, MA 02138

<sup>2</sup>Department of Astronomy, University of California Berkeley, Berkeley, CA 94720

<sup>3</sup>Alfred P. Sloan Research Fellow

<sup>4</sup>Cerro Tololo Inter-American Observatory (CTIO), Colina el Pino S/N, La Serena, Chile

<sup>5</sup>Physics Department, Harvard University, 17 Oxford Street, Cambridge, MA 02138

34 SNe Ia have standard  $H$ -band magnitudes with an RMS scatter of 0.15 mag. The good match of our sample with the literature sample suggests there are few systematic problems with the photometry. We present a nearby NIR Hubble diagram that shows no correlation of the residuals from the Hubble line with light-curve properties. Future samples that account for optical and NIR light-curve shapes, absorption, spectroscopic variation, or host-galaxy properties may reveal effective ways to improve the use of SNe Ia as distance indicators. Since systematic errors due to dust absorption in optical bands remain the leading difficulty in the cosmological use of supernovae, the good behavior of NIR light curves and the small sensitivity to reddening make rest-frame NIR measurements of SNe Ia attractive candidates for future cosmological work.

*Subject headings:* distance scale – supernovae: general

## 1. Introduction

Type Ia supernovae (SNe Ia) observed at optical wavelengths in the rest frame have played a leading role in extragalactic astronomy and cosmology in the past decade. SNe Ia have been the key to measuring the Hubble constant (Freedman et al. 2001; Jha et al. 1999; Riess et al. 2005) and demonstrating cosmic acceleration (Riess et al. 1998; Perlmutter et al. 1999). These discoveries rest on a foundation of photometric and spectroscopic similarities between high and low redshift SNe Ia (Hamuy et al. 1996; Riess et al. 1999; Goldhaber et al. 2001; Hook et al. 2005; Blondin et al. 2006; Jha et al. 2006; Conley et al. 2006; Garavini et al. 2007; Garg et al. 2007; Bronder et al. 2007; Foley et al. 2007; Ellis et al. 2007). The history of cosmic expansion has been traced out to redshift  $z \sim 1$  (Tonry et al. 2003; Knop et al. 2003; Barris et al. 2004). The predicted turnover to the matter-dominated era and the corresponding deceleration at  $z > 1$  has been seen by space-based work from *HST* (Riess et al. 2007). Two current projects: ESSENCE (Equation of State: SuperNova trace Cosmic Expansion; Miknaitis et al. 2007; Wood-Vasey et al. 2007), and SNLS (SuperNova Legacy Survey; Astier et al. 2006) seek to constrain the nature of the dark energy responsible for cosmic acceleration by measuring the equation-of-state parameter  $w$  with large, homogeneous samples of SNe Ia. ESSENCE and SNLS data are both consistent with dark energy described by a cosmological constant,  $w = -1.0$  to better than  $\pm 0.1$ .

These cosmological results are based on measurements of optical emission in the supernova rest frame, but recent work suggests that SNe Ia may be superior distance indicators in the near infrared (NIR), with a narrow distribution of peak  $JHK_s$  magnitudes and 4–8 times less sensitivity to reddening (Meikle 2000; Krisciunas et al. 2004a, 2007). Redden-

ing and absorption of supernova light by dust in their host galaxies poses the single most vexing systematic question facing SN Ia cosmology (Wang et al. 2006; Conley et al. 2007). Avoiding these complications would be very desirable, if the properties of the supernovae permit. These questions can be approached by building a homogeneous and large set of NIR observations. This paper is a step in that direction.

Early NIR observations of SNe Ia were made by Kirshner et al. (1973); Elias et al. (1981, 1985); Frogel et al. (1987), with more recent  $JHK_s$  light curves published by Jha et al. (1999); Hernandez et al. (2000); Valentini et al. (2003); Candia et al. (2003); Krisciunas et al. (2000, 2001, 2003, 2004b,c, 2005, 2006, 2007); Phillips et al. (2006); Pastorello et al. (2007); Stritzinger & Sollerman (2007); Wang et al. (2007); Elias-Rosa et al. (2007). Northern hemisphere work from the CfA Supernova Program uses observations from the robotic 1.3-m Peters Automated InfraRed Imaging TELEscope (PAIRITEL; Bloom et al. 2006) at Mount Hopkins, Arizona. The IR observations are part of a systematic program of supernova observations that includes dense sampling of supernova spectra (Matheson 2007) and concurrent  $UBVri$  optical photometry (Hicken et al. 2008, *in prep.*). This paper is a first report on the NIR data on SNe Ia from PAIRITEL. Similar work is underway in the southern hemisphere by the Carnegie Supernova Project using observations at the Las Campanas Observatory in Chile (Freedman 2005; Hamuy et al. 2006). The prospect of large homogeneous data sets coupled with progress in modeling SN Ia NIR light curves (Kasen 2006) raises hopes that SNe Ia, especially in the rest-frame  $H$  band, can be developed into the most precise and accurate of cosmological distance probes.

Recent work by Krisciunas et al. (2004a) shows that SNe Ia have a narrow range of luminosity in  $JHK_s$  at the time of  $B$ -band maximum light ( $t_{B\max}$ ) with smaller scatter than the  $B$  and  $V$  bands. Krisciunas et al. (2004a) found no correlation between optical light-curve shape and intrinsic IR luminosity. The NIR behavior is a sharp contrast to optical light curves, where a variety of ingenious methods have been devised to reduced the scatter in distance estimates: the  $\Delta m_{15}$  method (Hamuy et al. 1996; Phillips et al. 1999), the multicolor light-curve shape method (MLCS; Riess et al. 1996, 1998; Jha et al. 2006), the “stretch” method (Perlmutter et al. 1997; Goldhaber et al. 2001), the color-magnitude intercept calibration method (CMAGIC; Wang et al. 2003), and the spectral adaptive template method (SALT; Guy et al. 2005; Astier et al. 2006; Guy et al. 2007). For a sample of 16 SNe Ia observed in NIR bands, Krisciunas et al. (2004a) found a RMS of  $\sigma_J = 0.14$ ,  $\sigma_H = 0.18$ , and  $\sigma_{K_s} = 0.12$  mag. We set out to construct an independent set of observations to test this remarkable result.

In this paper we present 17 SNe Ia observed with PAIRITEL from 2005–2007. The 1065 individual data points in this sample represent the largest homogeneous set of SNe Ia to date,

tripling the NIR SN Ia observations in the literature. Data collection with PAIRITEL is discussed in §2. Data analysis, including the mosaic creation process and our photometry pipeline, is discussed in §3. We construct NIR  $JHK_s$  templates from this new sample as detailed in §4 and fit these templates to the SN Ia light curves to derive the  $JHK_s$  magnitudes at the time of  $B$ -band maximum light. These magnitudes are remarkably uniform, particularly in the  $J$  and  $H$  bands. Distances are calculated in §5, and we discuss the standard magnitude of NIR SNe Ia in §6. We then compare our sample to that compiled in Krisciunas et al. (2004a) as well as to some more recent SNe Ia from Pastorello et al. (2007) and Stanishev et al. (2007) in §7 and show that the  $J$  and  $H$  bands at maximum light, even from this heterogeneous sample, have a small range in absolute magnitude. Our conclusions are summarized in §8.

## 2. Data

We present 1065 near-infrared (NIR) measurements of 19 nearby SNe Ia obtained from 2005 to 2007 using the f/13.5 1.3-m PAIRITEL at the F.L. Whipple Observatory on Mount Hopkins, AZ. (Table 1). Dedicated in October 2004, PAIRITEL uses the northern telescope of the Two Micron All Sky Survey (2MASS; Skrutskie et al. 2006) together with the 2MASS southern camera. PAIRITEL is a fully automated, robotic telescope with the sequence of observations controlled by an intelligent queue-scheduling database (Bloom et al. 2006). Two dichroics allow simultaneous observing in  $JHK_s$  (1.2, 1.6, and 2.2  $\mu\text{m}$ ; Cohen et al. 2003) with three 256 $\times$ 256 pixel HgCdTe NICMOS3 arrays. The image scale of 2''/pixel provides a field of view of 8.53' $\times$ 8.53' for each filter. Since the supernova observations are conducted with the instrument that defines the 2MASS photometric system, we use the 2MASS point source catalog (Cutri et al. 2003) to establish the photometric zeropoints. Images are obtained with standard double-correlated reads with the long (7.8 sec) minus short (51 msec) frames in each filter treated as the “raw” frame in the reduction pipeline. The telescope is dithered ( $< 2'$ ) every fourth exposure to aid with reductions.

The CfA Supernova Program used PAIRITEL to follow up SNe discovered by optical searches at  $\delta \gtrsim -30$  degrees with  $V \lesssim 18$  mag. These are objects for which we routinely obtain extensive data sets of optical spectra and CCD photometry using other instruments at Mount Hopkins. With  $\sim 30\%$  of the time on this dedicated robotic telescope available for supernova observations, we observe  $\sim 3$ – $5$  SNe per night, and obtain host galaxy template reference images for each supernova. The first published PAIRITEL supernova observations were of the unusual core-collapse SN 2005bf (Tominaga et al. 2005). A detailed discussion of the observations presented here will be presented in Friedman et al. (2008), *in prep.*, but

we present a brief sketch of the data analysis path in the next section.

### 3. Data Analysis

Data were processed with one of two mosaicking pipelines. For fields dominated by large galaxies, we used a pipeline (see Modjaz 2007; Kocevski et al. 2007), which makes use of a bank of existing sky frames. For all other fields, we used the standard pipeline (see §3.1). Both pipelines process the 100–150 images, each of 7.8 seconds duration, by flat correction, dark and sky subtraction, registration, and stacking to create a final mosaicked image in each of the  $JHK_s$  filters. Mosaicked images typically comprise 3 images at each dither position, with a mosaicked FOV of  $\sim 12' \times 12'$ . The raw images are converted into final mosaics with  $1''/\text{pixel}$  sampling. Typical 1800-second observations (including slew overhead) reach magnitude limits of  $\sim 18, 17.5, 17$  mag for  $J, H,$  and  $K_s$ , respectively.

#### 3.1. Mosaics

The PAIRITEL camera has no shutter, so dark current cannot be measured independently, and background frames include both sky and dark photons (“skark”). PAIRITEL supernova observations did not include pointings that alternate between the source and the sky, so skark frames were created for each mosaic.

For large host galaxies with angular size  $\gtrsim 2'$  (in the  $12'$  FOV), host galaxy contamination prevents a reliable calculation of the skark background calculated from a pixel-by-pixel median through the stack of dithered images. Here skark frames are estimated using a median match to an archive of skark frames in relatively empty fields observed on the same night. The archival skark image is selected as close in time to the supernova observations as possible, with a median matched in a  $50 \times 50$  pixel box, known to have stable pixel properties, in the lower left quadrant of the array. After the dark plus sky frame is subtracted, images are mosaicked using the drizzle technique (Fruchter & Hook 2002).

For well-isolated supernovae with host galaxies of angular size  $\lesssim 2'$  (in a  $12'$  FOV), skark frames can be constructed from the science images themselves. This is done by applying a spline fit to a complete time series of sky values in each pixel for that observation. Since the fitting characteristics of the spline curve vary by filter, elevation, and weather, parameters are adjusted to best fit each observation and filter. The spline fit parameters define a function that tracks the time variation of the skark background in each of the  $256 \times 256$  pixels over the duration of the dither pattern. We construct a skark image at the time of each 7.8-second

science exposure by calculating the skark value in each pixel at this time and subtract that skark image from the science image. For cases where the galaxy occupies a small fraction of the field, this process improves the sky subtraction. This standard pipeline works better than simply taking the pixel-by-pixel median through the dithered (unregistered) stack of science images because it samples the sky variation on time scales that are shorter than the total exposure time. Mosaicked images are constructed using SWarp (Bertin 2005).

Most of our objects were reduced with the standard processing code. Only SN 2005cf, SN 2005ke, SN 2005na, SN 2006D, and SN 2006X required the large galaxy approach. For both methods, bad pixel masks and flat fields were created from archival images. See Fig. 1 for an example of a final  $JHK_s$  color mosaic created in the standard processing mode. Friedman et al. (2008) will contain a more detailed description of the mosaic creation process.

### 3.2. Photometry

Mosaicked images were fed to the photometry pipeline we have used in the ESSENCE and SuperMACHO projects (Rest et al. 2005; Garg et al. 2007; Miknaitis et al. 2007). This pipeline determines the noise based on the sky noise in the mosaic images, registers the images for a supernova to a common reference frame, and performs point-spread function (PSF) photometry using DoPHOT (Schechter et al. 1993). The 2MASS catalog (Cutri et al. 2003) is the natural astrometric and photometric reference system for these observations. In a typical  $12' \times 12'$  field of view, there were 10–100 2MASS stars in each filter. These stars were sufficient to calibrate the images to the 2MASS system  $JHK_s$  firmly enough that the underlying uncertainty in the 2MASS system, of about 3%, is the dominant error in the photometric calibrations for the light curves presented here. Cohen et al. (2003) describe the 2MASS  $JHK_s$  filter system in detail and Leggett et al. (2006) provide color transformations to put observations with the 2MASS filter system on other widely used photometric systems.

Final reference images were taken for each galaxy after the supernova had faded. DoPHOT photometry on the images was used for those SNe Ia that were clearly separated from their host galaxy and had little underlying contaminating light (SN 2005ao, SN 2005cf, SN 2005el, SN 2005hk, SN 2005ke, SN 2005eu, SN 2005iq, SN 2005na, SN 2006N, and SN 2006X). For these cases the galaxy light in the DoPHOT PSF at the location of the supernova in the reference images was subtracted from the supernova flux. In every case, the contribution from underlying galaxy light was less than 10% of the SN Ia light at maximum. Seeing at PAIRITEL is limited by the dome seeing and remains relatively constant from 1.8–2.0". The good effect of this mediocre dome seeing is that the contaminating galaxy light within the PSF is very nearly constant.

We used subtraction-based photometry (following Miknaitis et al. (2007)) for SNe Ia that were not clearly separated from their host galaxy. The NN2 method of Barris et al. (2005) was employed (as used in Miknaitis et al. 2007) by subtracting all  $N \times (N-1)/2$  unique pairs of images to minimize the sensitivity to subtraction errors. Because our PAIRITEL data are not critically sampled, the reliability of the PAIRITEL image subtraction is not as good as the subtractions in Miknaitis et al. (2007). Our photometric pipeline automatically detected and screened out subtractions with significant residual flux in known stars, leaving us with fewer high-quality light-curve points than would have been obtained in the case of perfect subtractions. For the supernovae where the underlying galaxy contribution was a small fraction of the supernova light, direct photometry on the unsubtracted images proved preferable.

Photometry was extracted from either the unsubtracted or the subtracted images by forcing DoPHOT to measure the PSF-weighted flux of the object at a fixed position. This position was determined in the  $J$ -band difference images that had a signal-to-noise ratio  $> 5$ . This average position was used for fixed-position DoPHOT photometry of each image of a SN Ia.

Flux measurements were calibrated to the 2MASS system by using photometric solutions to the 2MASS catalogs (Cutri et al. 2003). For the difference images the calibrated zeropoint from the template was used, with suitable correction for the convolution of the template image as detailed by Miknaitis et al. (2007).

#### 4. IR Template

We constructed  $JHK_s$  templates using the IR light curves from the PAIRITEL observations (presented in Table 3), the MLCS2k2.v004 (Jha et al. 2006) values fit to our own CCD observations (Hicken et al. 2008) for the time of  $B$ -band maximum light,  $t_{B\max}$ , and an initial guess for the  $H$ -band magnitude at  $t_{B\max}$ ,  $H_{B\max}$ .<sup>1</sup>

In constructing the templates, we excluded two SNe Ia from our overall sample of 19 SNe Ia: SN 2005hk and SN 2005ke. SN 2005hk is known to be an unusual SN Ia (Phillips et al. 2007; Sahu et al. 2007). SN 2005ke is a 1991bg-like SN Ia with possible circumstellar interaction (Patat et al. 2005; Immler et al. 2006). Both SN 2005hk and SN 2005ke exhibit only one infrared hump instead of the two exhibited by normal SNe Ia. The  $JHK_s$  maximum

---

<sup>1</sup>The IDL routines used to construct and fit these IR templates will be available in the online edition and at [http://www.cfa.harvard.edu/~sim\\$wmwood-vasey/IR/](http://www.cfa.harvard.edu/~sim$wmwood-vasey/IR/).

for these "dromedary" light curves occurs after the  $B$ -band maximum light, unlike normal "bactrian" SNe Ia for which the first IR maxima occur 3–5 rest-frame days before  $B$ -band maximum light. We compare our SN Ia  $H$ -band template to SN 2005ke and SN 2005hk in Fig. 3. Because we have excluded these two objects, our template does not extend to 1991bg-like SNe Ia or other unusual SNe Ia. This seems a reasonable approach while the data set is small. Unusual supernovae can be identified from a NIR light curve alone, or they can be identified from their optical spectra and light curves which we obtain as a matter of course. In any case, we defer incorporating these unusual objects into a more comprehensive treatment of NIR lightcurves until the available database of near-infrared SN Ia light curves is more fully populated.

The IR light curves for the remaining 17 SNe Ia were registered to a common phase by subtracting  $t_{B\max}$  and accounting for time dilation based on the heliocentric redshift,  $z_{\text{helio}}$  (Leibundgut et al. 1996; Goldhaber et al. 2001). The SN Ia lightcurves were then registered to a common magnitude scale by subtracting the initial guess for  $H_{B\max}$  determined by rough visual inspection of the light curve (the fitting process is insensitive to the determination of the initial  $H_{B\max}$  guess to within  $\pm 0.5$  mag). Unlike Krisciunas et al. (2004a), we do not further adjust this phase by the optical light-curve width parameter. We found that compensating for the light-curve width gave no improvement in the template fits or in the resulting dispersion of absolute magnitudes (see §6) determined between -10 and +20 days in phase. However, the position of the second IR maximum is variable, and may be related to intrinsic luminosity. In larger data sets it will be worth exploring whether a width-correction parameter would produce a more effective template for fitting the second maximum at later times.

This initial set of standardized light curves was sampled on a daily basis from  $-20$  to  $+80$  days and then fit with the IDL routine "INTERPOL". This interpolation was smoothed twice with a boxcar of length 5 days. The smoothing has very little effect near maximum light because of our dense sampling at those epochs. Varying the smoothing length between 1 and 5 days did not substantially affect the template near maximum. However, at late times ( $+30$  days), we found some smoothing necessary because we had fewer points from which to construct the template.

To refine this template, we determined the magnitude value at  $t_{B\max}$  that minimized the  $\chi^2$  of the template versus the data over the span from  $[-10, +20]$  days. These new magnitude offsets were then used to seed the process above where we had previously used the initial guesses for  $H_{B\max}$ . The procedure was iterated twice more to construct final values at  $t_{B\max}$  for each SN Ia, and the final template was constructed based on these values. We found that three iterations were sufficient to reach convergence. The uncertainty in the template



is the standard deviation of the residuals of the SN Ia light-curve points around the mean template in a moving 5-day window. This procedure was performed for each of the  $JHK_s$  IR passbands. For our data, the  $H$ -band light curve was observed to exhibit small scatter from  $[-10, +40]$  days. The  $J$ -band aggregate light curve has small scatter about the template from  $[-10, +10]$  days but begins to show variations in the time and flux of the secondary maximum for individual supernovae. The  $K$ -band data from our PAIRITEL observations is not as good as the  $J$ - and  $H$ -band data due to increased sky background in  $K$ . Our template in the  $K$  band shows significantly more scatter with fewer objects. We draw no firm conclusions in this paper with regard to  $K$ -band SN Ia light curves.

The unusual cases that were excluded from the template construction are easily seen to be far from the  $H$ -band template. Fitting either SN 2005hk or SN 2005ke with the PAIRITEL SN Ia  $H$ -band template results in a sufficiently bad  $\chi^2/\text{DoF}$  ( $> 10$ ) that these SNe Ia would be excluded based on that criterion alone.

Future work will include a  $K$ -correction for the IR photometry (cf. Krisciunas et al. 2004b,c), but this sample only extends to redshift of  $z \sim 0.03$  where the effect of  $K$ -corrections is small (Krisciunas et al. 2004b).

## 5. Galaxy Redshifts

Recession velocities for our SNe Ia are those of the identified host galaxies in the NASA/IPAC Extragalactic Database (NED)<sup>2</sup>. We use the quoted velocity with respect to the Virgo infall model of Mould et al. (2000). For SNe Ia within  $3000 \text{ km s}^{-1}$  we used available information on distances to the galaxies to minimize our sensitivity to the details of the local flows. We used the values of Krisciunas et al. (2004a,b) for SN 1998bu and SN 2002bo and Wang et al. (2007) for SN 2006X. After accounting for these SNe Ia, we were left with two SNe Ia within  $3000 \text{ km s}^{-1}$  for which we used the Mould et al. (2000) values, SN 2005cf and SN 2006D. Outside of  $3000 \text{ km s}^{-1}$  differences among various flow models are not significant. One supernova, SN 1999cl, occurred in a Virgo cluster member galaxy, NGC 4501, so we used the Virgo cluster redshift instead of the recession velocity of NGC 4501. We assumed a peculiar velocity of  $\sigma_{\text{vel}} = 150 \text{ km s}^{-1}$  (Radburn-Smith et al. 2004) and the redshift measurement uncertainty for each host galaxy as reported by NED. These uncertainties were converted into a distance modulus uncertainty,  $\sigma_{\mu}(\text{vel})$ , using Eq. 1.

$$\sigma_{\mu}(\text{vel}) = \frac{(5 \ln 10)^2}{z^2} \sqrt{\sigma_{\text{vel}}/c^2 + \sigma_z^2} \quad (1)$$

---

<sup>2</sup><http://nedwww.ipac.caltech.edu/>

This is valid for a smooth cosmology that resembles any currently allowed cosmological expansion model. Values for  $\sigma_\mu(\text{vel})$  for the SNe Ia considered in this paper are given in column 12 of Table 2.

We confirmed the NED heliocentric redshift values with the heliocentric galaxy redshifts derived from spectra of the hosts as observed by the CfA Supernova Program<sup>3</sup> and measured using the galaxy redshift code RVSAO (Kurtz & Mink 1998). All were consistent with the NED values within 200 km s<sup>-1</sup>. For SN 2007cq, no NED redshift was available for the host galaxy so we used the value from the CfA galaxy spectrum as the heliocentric velocity and then used the Mould et al. (2000) model conversion provided by NED to express this redshift in the CMB+Virgo infall frame.

## 6. Distance Moduli and the Standard IR Brightness of SNe Ia

The most uniform behavior of our SN Ia light curves is in the  $H$ -band, and that band is where we focus our analysis. In the most simplistic treatment, we take the  $H_{\text{Bmax}}$  for each SN Ia to have a standard value. Then the distance modulus is simply:

$$\mu = H_{\text{Bmax}} - M_{H_{\text{Bmax}}} \quad (2)$$

where  $M_{H_{\text{Bmax}}}$  is the absolute  $H$ -band magnitude of a SN Ia at  $B$ -band maximum light. The numerical value for the absolute magnitude of SNe Ia in  $H$  is separate from the question of how well the  $H$ -band magnitudes trace cosmic expansion.

The set of redshifts, apparent magnitudes, and accompanying uncertainties from §5 were compared to a  $\Lambda$ CDM concordance cosmology ( $\Omega_M, \Omega_\Lambda, w$ )=(0.27, 0.73, -1). We solve for the absolute mean brightness of a SN Ia in  $H$ -band at  $B$ -band maximum light by taking the weighted mean of the differences of the apparent magnitudes and the  $\Lambda$ CDM distance moduli (the exact cosmology doesn't quantitatively affect the results at these redshifts):

$$M_{H_{\text{Bmax}}} = \sum_{i=1}^N \frac{H_{\text{Bmax}}^i - \mu^i}{\sigma_{H_{\text{Bmax}}}^i + \sigma_{\mu(\text{vel})}^i} \bigg/ \sum_{i=1}^N \left( \sigma_{H_{\text{Bmax}}}^i + \sigma_{\mu(\text{vel})}^i \right)^2 \quad (3)$$

Assuming an  $H_o$  of 72 km s<sup>-1</sup> Mpc<sup>-1</sup> (Freedman et al. 2001; Spergel et al. 2003, 2007) we find  $M_{H_{\text{Bmax}}} = -17.98 \pm 0.03$  for the fiducial  $H$ -band magnitude at  $B$ -band maximum light. A similar analysis for the  $J$ -band magnitude at  $B$ -band maximum light finds  $M_{J_{\text{Bmax}}} = -18.34 \pm 0.04$  with an RMS of 0.36 mag.

---

<sup>3</sup><http://www.cfa.harvard.edu/supernova/RecentSN.html>

For a cosmological fit one would marginalize over the combination

$$\mathcal{M}_{H_{\text{Bmax}}} = M_{H_{\text{Bmax}}} - 5 \log_{10} h_o + 15 + 5 \log_{10} c \quad (4)$$

$$\sigma_{\mathcal{M}_{H_{\text{Bmax}}}} = 5 \frac{\sigma_{h_o}}{h_o} \log_{10} e \quad (5)$$

where  $h = H_o/(100 \text{ km s}^{-1} \text{ Mpc}^{-1})$  and  $c$  is the speed of light in vacuum in  $\text{km s}^{-1}$ . The marginalization in our case is trivial because we are assuming a fixed  $\Lambda$ CDM cosmology. This assumption allows us to propagate a  $H_o$  uncertainty of 10% directly through Eq. 5 to determine our global uncertainty in  $M_{H_{\text{Bmax}}}$ . The mean value of  $M_{H_{\text{Bmax}}}$  is unchanged by the marginalization, but the total uncertainty is increased to  $\pm 0.22$ . It is the uncertainty in  $H_o$  that dominates in the global uncertainty for  $M_{H_{\text{Bmax}}}$ .

Small variation in the NIR absolute magnitudes of SNe Ia is an important result that was first found by Krisciunas et al. (2004a). Here, we have an independent confirmation of this result from a homogeneous set of well-sampled SNe Ia light curves observed with PAIRITEL. In the next section, we expand that data set by joining the PAIRITEL sample with SNe Ia from the literature.

## 7. Comparison with Literature SNe Ia

We joined our PAIRITEL sample with 17 SNe Ia from the literature (see Table 2) extending back to SN 1998bu (earlier observations of supernovae with earlier detectors were not included in this study). We generated a new set of IR templates following the same prescription as in § 4 and found that the full sample of SNe Ia was just as well-behaved as the PAIRITEL sample. This is a tribute to the care of the observers and the clear definition of the 2MASS photometric system. The NIR SN Ia templates and associated standard deviations for this combined sample are shown in Fig. 2. The small scatter of the  $H$ -band light curves from  $[-10, +20]$  days and the  $J$ -band light curves from  $[-10, +10]$  days was preserved in the heterogeneous sample. Fig. 4 shows the tight scatter of the  $H$ -band SN Ia light-curve data points around the fiducial template.

We present the  $H$ -band apparent magnitudes from this global template in Table 2. The comparison of these apparent magnitudes with the expected luminosity distance relation of a  $\Lambda$ CDM cosmology,  $(\Omega_M, \Omega_\Lambda, h_o) = (0.3, 0.7, 0.72)$ , is shown in Fig. 5. We find a global  $H$ -band RMS of 0.15 mag around an absolute magnitude of  $M_H = -17.98 \pm 0.03$  (see Fig. 6). A similar analysis for  $J$ -band finds similar agreement with the PAIRITEL-only values with a global value of  $M_J = -18.32 \pm 0.04$  with an RMS of 0.28 mag. To check the quality of the light-curve fits and to see if the fits are robust, we plot the  $H$ -band residuals with

respect to the  $\chi^2/\text{DoF}$  and degrees of freedom of the fits to the  $H$ -band template in Fig. 7. Addressing concerns of correlation of residuals with SN Ia properties, Fig. 8 demonstrates that there is no correlation in the  $H$ -band residuals with the light-curve shape parameter,  $\Delta$ , or extinction,  $A_V$ , as measured from the optical light curves by MLCS2k2 (Jha et al. 2007).

To reduce the effects of uncertainties in the local flow, we also calculated the RMS for only the 28 SNe Ia with a CMB+Virgo infall model velocity of  $> 2000 \text{ km s}^{-1}$ . We found an RMS of 0.15 mag for this sample. Previous work by Radburn-Smith et al. (2004) and Neill et al. (2007) found that SN Ia distances were more consistent with the Hubble law when a local flow model was incorporated. Future work from larger samples of nearby SNe Ia in the NIR will allow for the investigation of both the local flow and the absolute NIR magnitudes of SNe Ia from integrated analyses with more sophisticated flow models of the local Universe.

## 8. Conclusions

We have presented a method to find accurate luminosity distances to SNe Ia using the  $H$ -band light curve from  $[-10, +20]$  days after  $B$ -band maximum light. Within the photometric and local-flow uncertainties, the distribution about a best-fit  $\Lambda\text{CDM}$  model is consistent with no intrinsic dispersion of our  $H$ -band template fit magnitude values. Even without accounting for peculiar velocity uncertainties, the RMS scatter of 0.15 mag from these *uncorrected* inferred luminosity distance moduli is as small as *corrected* distances from optical-based methods. No correction for extinction or light-curve shape has been made here. It is quite plausible that using information on the NIR and optical light-curve shapes, dust absorption as fit from the optical to the infrared, spectroscopic variation, or host-galaxy properties will result in even smaller scatter and better distance determinations.

The Krisciunas et al. (2004a) result was determined from an inhomogeneous sample of 16 light curves. This paper improves on that work by providing a homogeneous sample of 17 PAIRITEL SN Ia light curves that more than triples the number of independent photometric observations in the literature. With our ongoing program at Mt. Hopkins adding  $\sim 10\text{--}15$  SNe Ia per year, PAIRITEL will continue building an extensive nearby training set of ground-based NIR SNe Ia. While we observe all the SNe Ia that meet our criteria, objects in the Hubble flow observed with adequate integration times to beat down the measurement errors will be the most helpful.

In this paper, we considered reddening values derived from optical data, and found it unnecessary to apply reddening corrections in  $H$ -band for the objects in our sample.

However, recent work on the highly extinguished SN 2002cv (Elias-Rosa et al. 2007) shows that reddening corrections will be necessary for some highly-absorbed SNe Ia in the NIR. Reddening uncertainties derived from optical data alone currently represent the most significant systematic error affecting SN Ia luminosity distance measurements. Simulations by Krisciunas et al. (2007) demonstrate major improvements to be gained from the addition of NIR data. Krisciunas et al. (2007) show that simulated distance modulus errors are improved by factors of 2.7 and 3.5 by adding  $J$ , and  $JHK_s$  to  $UBVRI$  data, respectively (Krisciunas et al. 2007). Reducing systematics due to reddening are crucial to future space-based SN surveys which will be large enough to avoid limitations from sample size. In that case, improving the constraints on cosmological parameters will be limited by systematics. We will explore the utility of a full combination of optical and NIR data to more precisely measure and correct for reddening in Friedman et al. (2008).

Although ground-based NIR data can be obtained for low redshift objects, rest-frame NIR observations for high- $z$  SNe Ia will have to be done from space. Currently, rest-frame SN Ia Hubble diagrams of high- $z$  SNe Ia have yet to be constructed beyond the  $I$  band (Freedman 2005; Nobili et al. 2005), with limited studies of SNe Ia and their host galaxies conducted in the mid-infrared with Spitzer (Chary et al. 2005; Gerardy et al. 2007).

Because nearby SNe Ia are excellent standard candles in the NIR, it may be worth careful consideration of the rest-frame NIR for the space missions using SNe Ia for cosmology. For example, the SNAP (Aldering 2004) and DESTINY satellites (Lauer 2005), candidates for the NASA/DOE Joint Dark Energy Mission (JDEM) mission, are both currently designed with detectors sensitive out to  $1.7 \mu\text{m}$ , which will only detect rest-frame  $H$ -band light ( $1.6 \mu\text{m}$ ) out to  $z \sim 0.1$ . Only a detector capable of observing rest-frame  $H$ -band at  $z \sim 0.5\text{--}2$  could take full advantage of Nature’s gift to us of a superb standard candle in the rest frame  $H$ -band. Such a detector would require sensitivity from  $2\text{--}5 \mu\text{m}$ . We can look forward to work of this type with JWST, just over the horizon. The astronomical community should discuss which aspects of a JDEM mission could best be carried out in the rest-frame IR.

The Peters Automated Infrared Imaging Telescope (PAIRITEL) is operated by the Smithsonian Astrophysical Observatory (SAO) and was made possible by a grant from the Harvard University Milton Fund, the camera loan from the University of Virginia, and the continued support of the SAO and UC Berkeley. Partial support for PAIRITEL operations and this work comes from National Aeronautics and Space Administration (NASA) grant NNG06GH50G (“PAIRITEL: Infrared Follow-up for Swift Transients”). PAIRITEL support and processing is conducted under the auspices of a DOE SciDAC grant (DE-FC02-06ER41453), which provides support to J.S.B.’s group. J.S.B. thanks the Sloan Research Fellowship for partial support.

We gratefully made use of the NASA/IPAC Extragalactic Database (NED). This publication makes use of data products from the 2MASS Survey, funded by NASA and the US National Science Foundation (NSF). IAUC/CBET were useful. M.W.V. is funded by a grant from the US National Science Foundation (AST-057475). A.S.F. acknowledges support from an NSF Graduate Research Fellowship and a NASA Graduate Research Program Fellowship. M. M. acknowledges support in part from a Miller Research Fellowship. A.S.F, R.P.K, M.M., and S.B. thank the Kavli Institute for Theoretical Physics, which is supported by the NSF through grant PHY05-51164. The CfA Supernova Program is supported in part by NSF Grant AST 06-06772. C.B. acknowledges support from the Harvard Origins of Life Initiative.

## REFERENCES

- Aldering, G. 2004, in *Wide-Field Imaging From Space*
- Astier, P., et al. 2006, *A&A*, 447, 31
- Barris, B. J., et al. 2004, *ApJ*, 602, 571
- Barris, B. J., Tonry, J. L., Novicki, M. C., & Wood-Vasey, W. M. 2005, *AJ*, 130, 2272
- Bertin, E. 2005, SWarp (TeraPix. [http://terapix.iap.fr/rubrique.php?id\\_rubrique=49](http://terapix.iap.fr/rubrique.php?id_rubrique=49))
- Blondin, S., et al. 2006, *AJ*, 131, 1648
- Bloom, J. S., et al. 2006, in *Astronomical Society of the Pacific Conference Series, Vol. 351, Astronomical Data Analysis Software and Systems XV*, ed. C. Gabriel, C. Arviset, D. Ponz, & S. Enrique, 751–+
- Bronder, T. J., et al. 2007, ArXiv e-prints, 0709.0859
- Candia, P., et al. 2003, *PASP*, 115, 277
- Chary, R., Dickinson, M. E., Teplitz, H. I., Pope, A., & Ravindranath, S. 2005, *ApJ*, 635, 1022
- Cohen, M., Wheaton, W. A., & Megeath, S. T. 2003, *AJ*, 126, 1090
- Conley, A., Carlberg, R. G., Guy, J., Howell, D. A., Jha, S., Riess, A. G., & Sullivan, M. 2007, *ApJ*, 664, L13
- Conley, A., et al. 2006, *AJ*, 132, 1707
- Cutri, R. M., et al. 2003, 2MASS All Sky Catalog of point sources. (The IRSA 2MASS All-Sky Point Source Catalog, NASA/IPAC Infrared Science Archive. <http://irsa.ipac.caltech.edu/applications/Gator/>)
- Elias, J. H., Frogel, J. A., Hackwell, J. A., & Persson, S. E. 1981, *ApJ*, 251, L13
- Elias, J. H., Matthews, K., Neugebauer, G., & Persson, S. E. 1985, *ApJ*, 296, 379
- Elias-Rosa, N., et al. 2007, ArXiv e-prints, 0710.4503
- Ellis, R. S., et al. 2007, ArXiv e-prints, 0710.3896
- Foley, R. J., et al. 2007, ArXiv e-prints, 0710.2338

- Freedman, W. L., et al. 2001, *ApJ*, 553, 47
- Freedman, W. L. . T. C. S. P. 2005, in *ASP Conf. Ser. 339: Observing Dark Energy*, 50–+
- Friedman, A. S., Wood-Vasey, W. M., Kirshner, R. P., Hicken, M., & Modjaz, M. 2008
- Frogel, J. A., Gregory, B., Kawara, K., Laney, D., Phillips, M. M., Terndrup, D., Vrba, F., & Whitford, A. E. 1987, *ApJ*, 315, L129
- Fruchter, A. S., & Hook, R. N. 2002, *PASP*, 114, 144
- Garavini, G., et al. 2007, *A&A*, 470, 411
- Garg, A., et al. 2007, *AJ*, 133, 403
- Gerardy, C. L., et al. 2007, *ApJ*, 661, 995
- Goldhaber, G., et al. 2001, *ApJ*, 558, 359
- Guy, J., et al. 2007, *A&A*, 466, 11
- Guy, J., Astier, P., Nobili, S., Regnault, N., & Pain, R. 2005, *A&A*, 443, 781
- Hamuy, M., et al. 2006, *PASP*, 118, 2
- Hamuy, M., Phillips, M. M., Suntzeff, N. B., Schommer, R. A., Maza, J., Smith, R. C., Lira, P., & Aviles, R. 1996, *AJ*, 112, 2438
- Hernandez, M., et al. 2000, *MNRAS*, 319, 223
- Hicken, M., Wood-Vasey, W. M., Modjaz, M., & Kirshner, R. P. 2008
- Hook, I. M., et al. 2005, *AJ*, 130, 2788
- Immler, S., et al. 2006, *ApJ*, 648, L119
- Jha, S., et al. 1999, *ApJS*, 125, 73
- Jha, S., et al. 2006, *AJ*, 131, 527
- Jha, S., Riess, A. G., & Kirshner, R. P. 2007, *ApJ*, 659, 122
- Kasen, D. 2006, *ApJ*, 649, 939
- Kirshner, R. P., Willner, S. P., Becklin, E. E., Neugebauer, G., & Oke, J. B. 1973, *ApJ*, 180, L97+



- Knop, R. A., et al. 2003, ApJ, 598, 102
- Kocevski, D., et al. 2007, ApJ, 663, 1180
- Krisciunas, K., et al. 2007, AJ, 133, 58
- Krisciunas, K., Hastings, N. C., Loomis, K., McMillan, R., Rest, A., Riess, A. G., & Stubbs, C. 2000, ApJ, 539, 658
- Krisciunas, K., et al. 2001, AJ, 122, 1616
- Krisciunas, K., Phillips, M. M., & Suntzeff, N. B. 2004a, ApJ, 602, L81
- Krisciunas, K., et al. 2004b, AJ, 127, 1664
- Krisciunas, K., Prieto, J. L., Garnavich, P. M., Riley, J.-L. G., Rest, A., Stubbs, C., & McMillan, R. 2006, AJ, 131, 1639
- Krisciunas, K., et al. 2003, AJ, 125, 166
- Krisciunas, K., et al. 2004c, AJ, 128, 3034
- Krisciunas, K., et al. 2005, AJ, 130, 350
- Kurtz, M. J., & Mink, D. J. 1998, PASP, 110, 934
- Lauer, T. R. 2005, New Astronomy Review, 49, 354
- Leggett, S. K., et al. 2006, MNRAS, 373, 781
- Leibundgut, B., et al. 1996, ApJ, 466, L21+
- Matheson, T. *et al.* 2007, AJ, *submitted*
- Meikle, W. P. S. 2000, MNRAS, 314, 782
- Miknaitis, G., et al. 2007, ApJ, 666, 674
- Modjaz, M. 2007, PhD thesis, Harvard University
- Mould, J. R., et al. 2000, ApJ, 529, 786
- Neill, J. D., Hudson, M. J., & Conley, A. 2007, ApJ, 661, L123
- Nobili, S., et al. 2005, A&A, 437, 789
- Pastorello, A., et al. 2007, MNRAS, 376, 1301

- Patat, F., Baade, D., Wang, L., Taubenberger, S., & Wheeler, J. C. 2005, IAU Circ., 8631, 1
- Perlmutter, S., et al. 1999, ApJ, 517, 565
- Perlmutter, S., et al. 1997, ApJ, 483, 565
- Phillips, M. M., et al. 2006, AJ, 131, 2615
- Phillips, M. M., et al. 2007, PASP, 119, 360
- Phillips, M. M., Lira, P., Suntzeff, N. B., Schommer, R. A., Hamuy, M., & Maza, J. 1999, AJ, 118, 1766
- Radburn-Smith, D. J., Lucey, J. R., & Hudson, M. J. 2004, MNRAS, 355, 1378
- Rest, A., et al. 2005, ApJ, 634, 1103
- Riess, A. G., et al. 1998, AJ, 116, 1009
- Riess, A. G., et al. 1999, AJ, 117, 707
- Riess, A. G., et al. 2005, ApJ, 627, 579
- Riess, A. G., Press, W. H., & Kirshner, R. P. 1996, ApJ, 473, 88
- Riess, A. G., et al. 2007, ApJ, 659, 98
- Sahu, D. K., Tanaka, M., Anupama, G. C., Kawabata, K. S., Maeda, K., Tominaga, N., Nomoto, K., & Mazzali, P. A. 2007, ArXiv e-prints, 710
- Schechter, P. L., Mateo, M., & Saha, A. 1993, PASP, 105, 1342
- Skrutskie, M. F., et al. 2006, AJ, 131, 1163
- Spergel, D. N., et al. 2007, ApJS, 170, 377
- Spergel, D. N., et al. 2003, ApJS, 148, 175
- Stanishev, V., et al. 2007, A&A, 469, 645
- Stritzinger, M., & Sollerman, J. 2007, A&A, 470, L1
- Tominaga, N., et al. 2005, ApJ, 633, L97
- Tonry, J. L., et al. 2003, ApJ, 594, 1

Valentini, G., et al. 2003, ApJ, 595, 779

Wang, L., Goldhaber, G., Aldering, G., & Perlmutter, S. 2003, ApJ, 590, 944

Wang, L., Strovink, M., Conley, A., Goldhaber, G., Kowalski, M., Perlmutter, S., & Siegrist, J. 2006, ApJ, 641, 50

Wang, X., et al. 2007, ArXiv e-prints, 0708.0140

Wood-Vasey, W. M., et al. 2007, ApJ, 666, 694

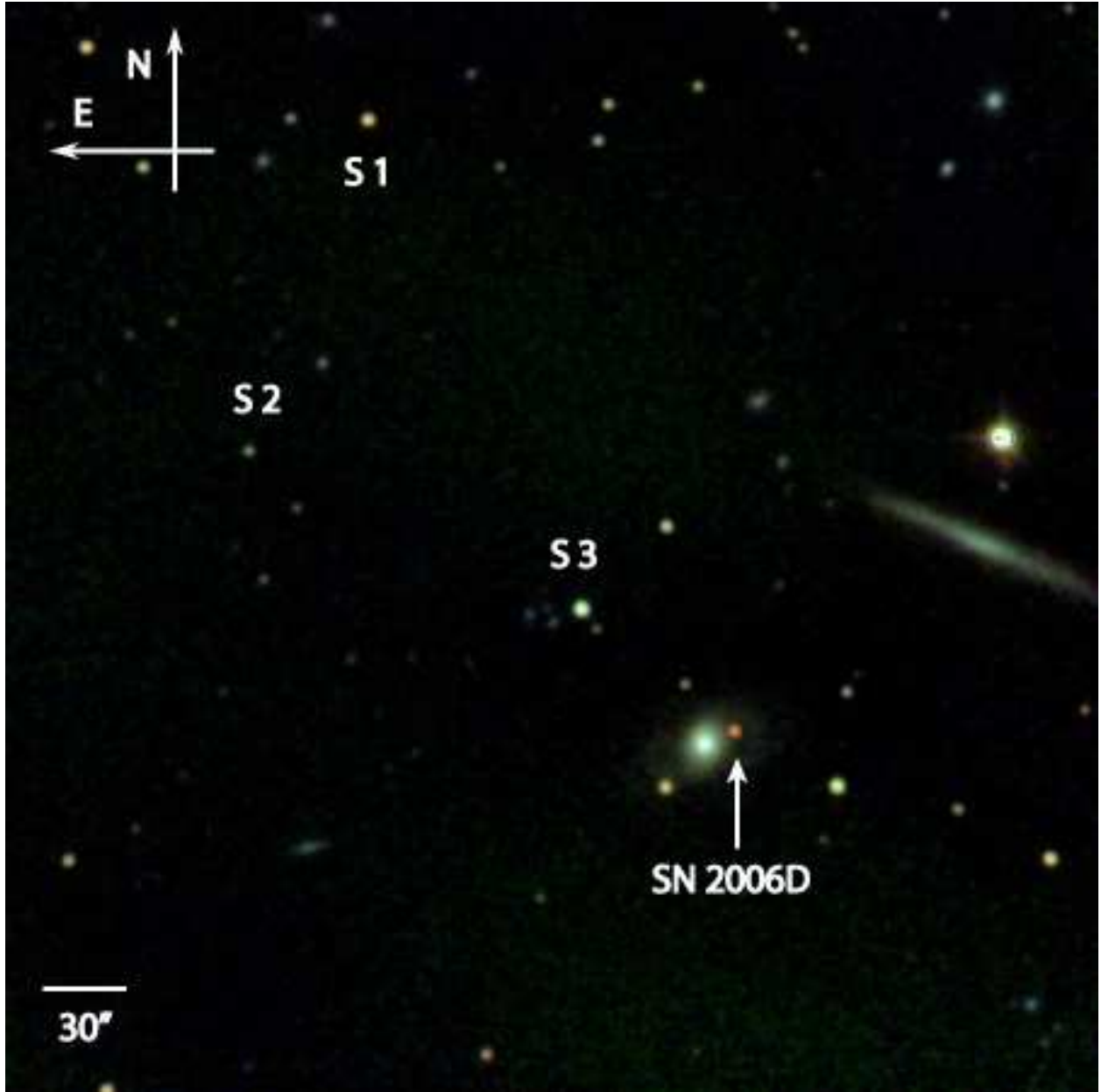


Fig. 1.— PAIRITEL  $JHK_s$  composite color image of SN 2006D (orange-red dot to upper right of galaxy in lower-right corner) at a week past maximum light when the SN Ia had IR magnitudes of  $(J, H, K) \cong (16.1, 14.8, 15.0)$ . The image shown is  $7.5' \times 7.5'$  in size. There are  $\sim 30$  2MASS stars in this field that were used for the photometric calibration of our PAIRITEL images of SN 2006D. The S1, S2, and S3 labels indicate three representative 2MASS stars with  $JHK_s$  magnitudes of S1: (14.11, 13.76, 13.71), S2: (16.02, 15.335, 14.830), and S3 (13.23, 12.61, 12.41).

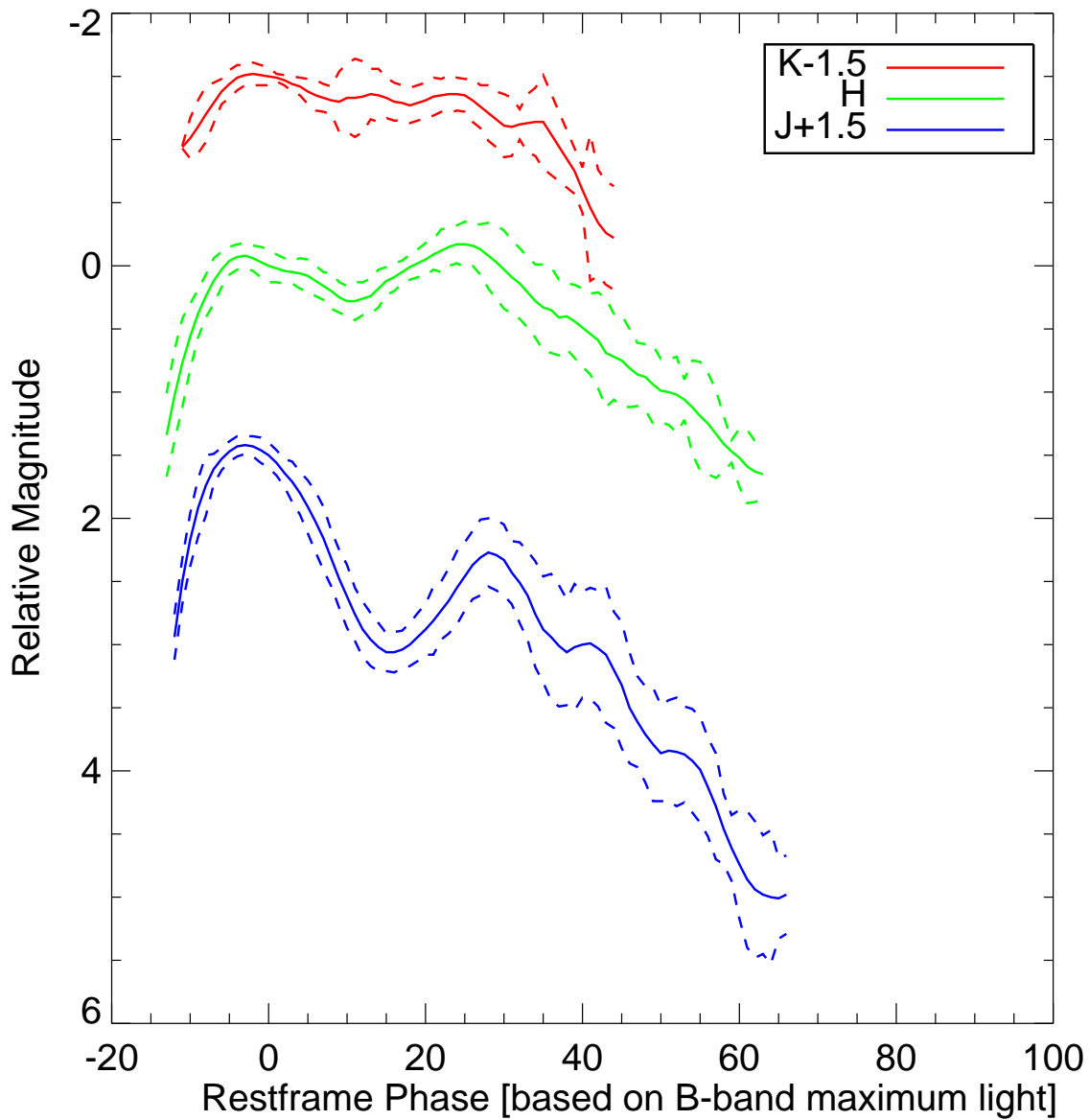


Fig. 2.— Infrared templates constructed from and then used to fit all of the NIR SNe Ia light curves considered in this paper (see §). The  $1\text{-}\sigma$  uncertainties (dashed lines) are based on the sample variance within a 5-day moving window of the SN Ia with respect to the fiducial template.

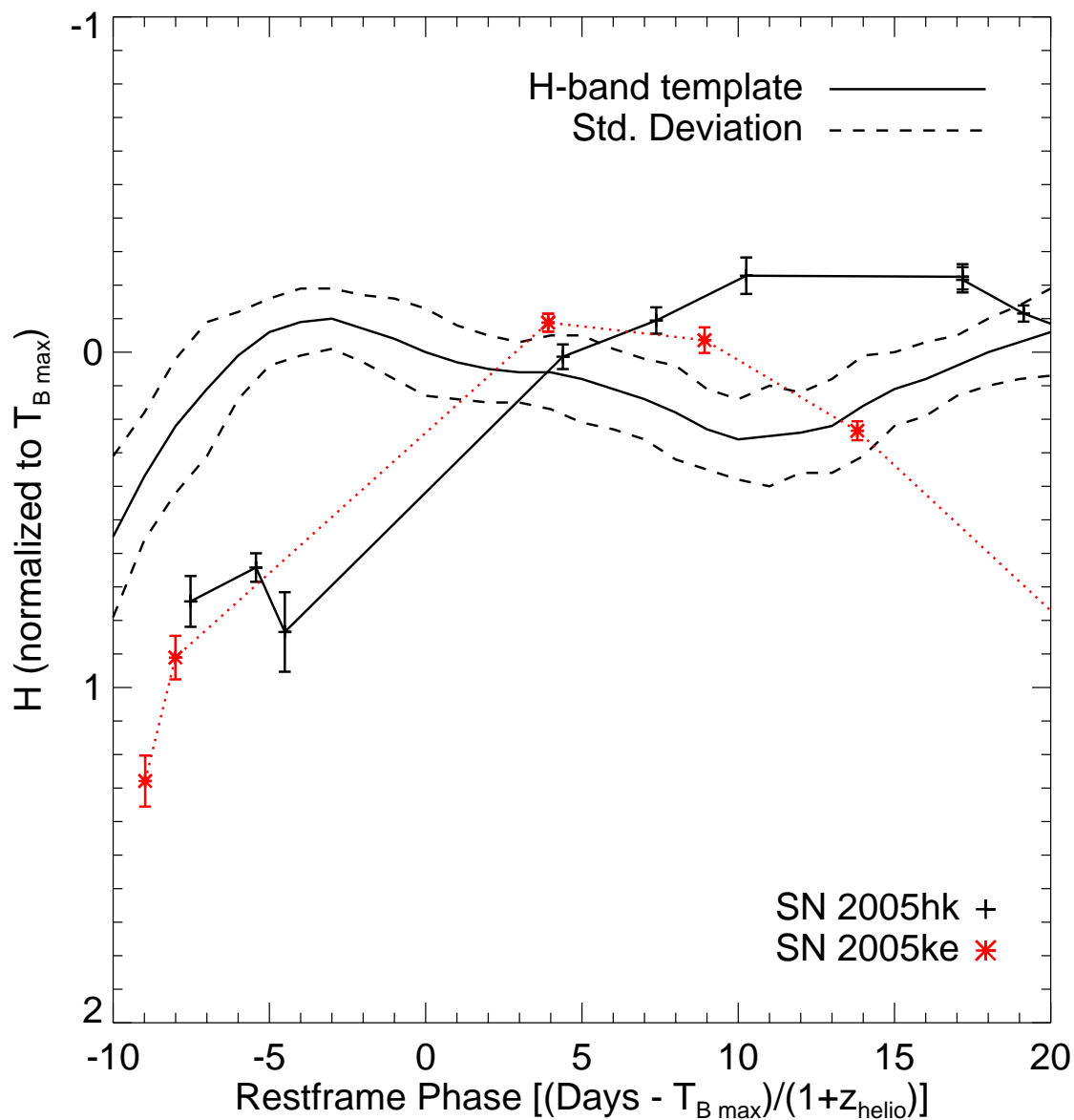


Fig. 3.— SN 2005hk and SN 2005ke were observed as part of the PAIRITEL campaign but were excluded from the construction of the template because they were known unusual SNe Ia. We compare their  $H$ -band light curves with the normal SN Ia  $H$ -band template to demonstrate the clarity with which these unusual supernovae can be distinguished from the normal SNe Ia used in the Hubble diagram.

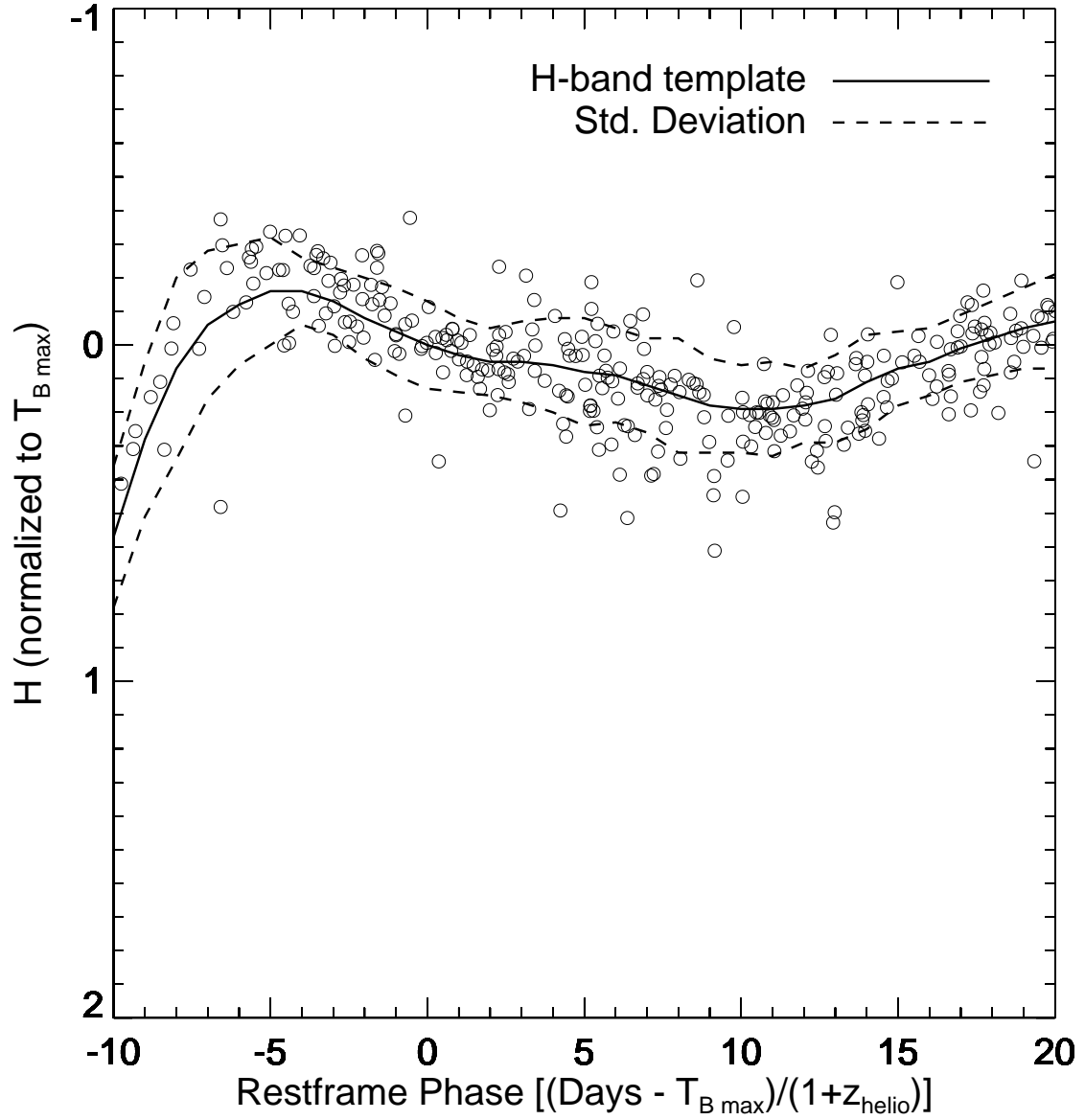


Fig. 4.— NIR  $H$ -band template based on all of the SNe Ia considered in this paper together with the constituent SN Ia observations. Model uncertainties are indicated by dashed lines as in Fig. 2.

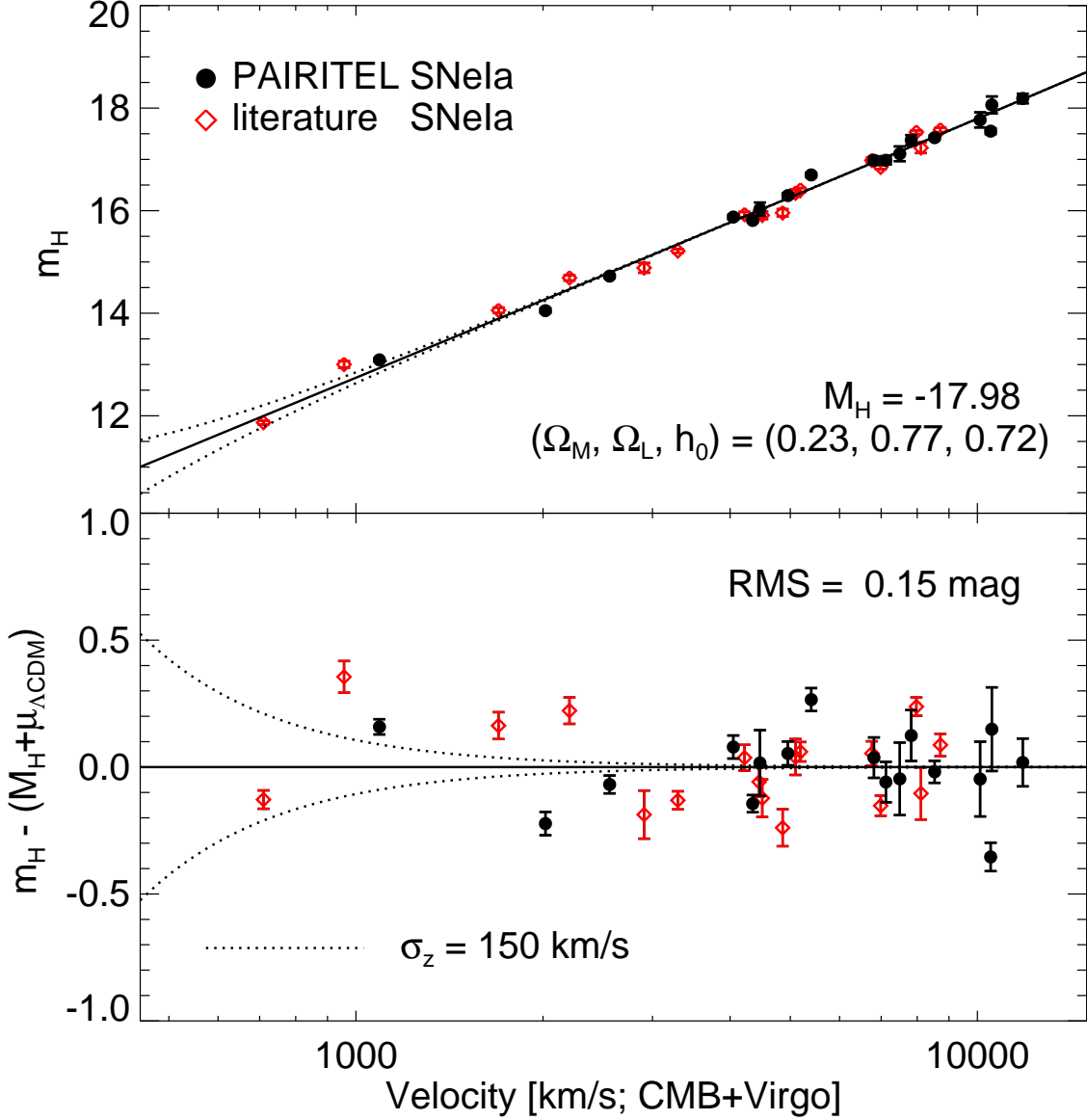


Fig. 5.—  $H$ -band SN Ia Hubble Diagram ( $\mu_H$  vs.  $z$  and residual vs.  $z$ ). RMS dispersion of 0.15 mag. SNe Ia from the literature are shown as open diamonds while the new SNe Ia from this paper are shown as filled circles. The error bars are the fit uncertainties from the fit to the  $H$ -band template (column 7 of Table 2). The reduced Hubble constant,  $h_o$ , is  $h_o = H_o/100 \text{ km s}^{-1} \text{ Mpc}^{-1}$ .



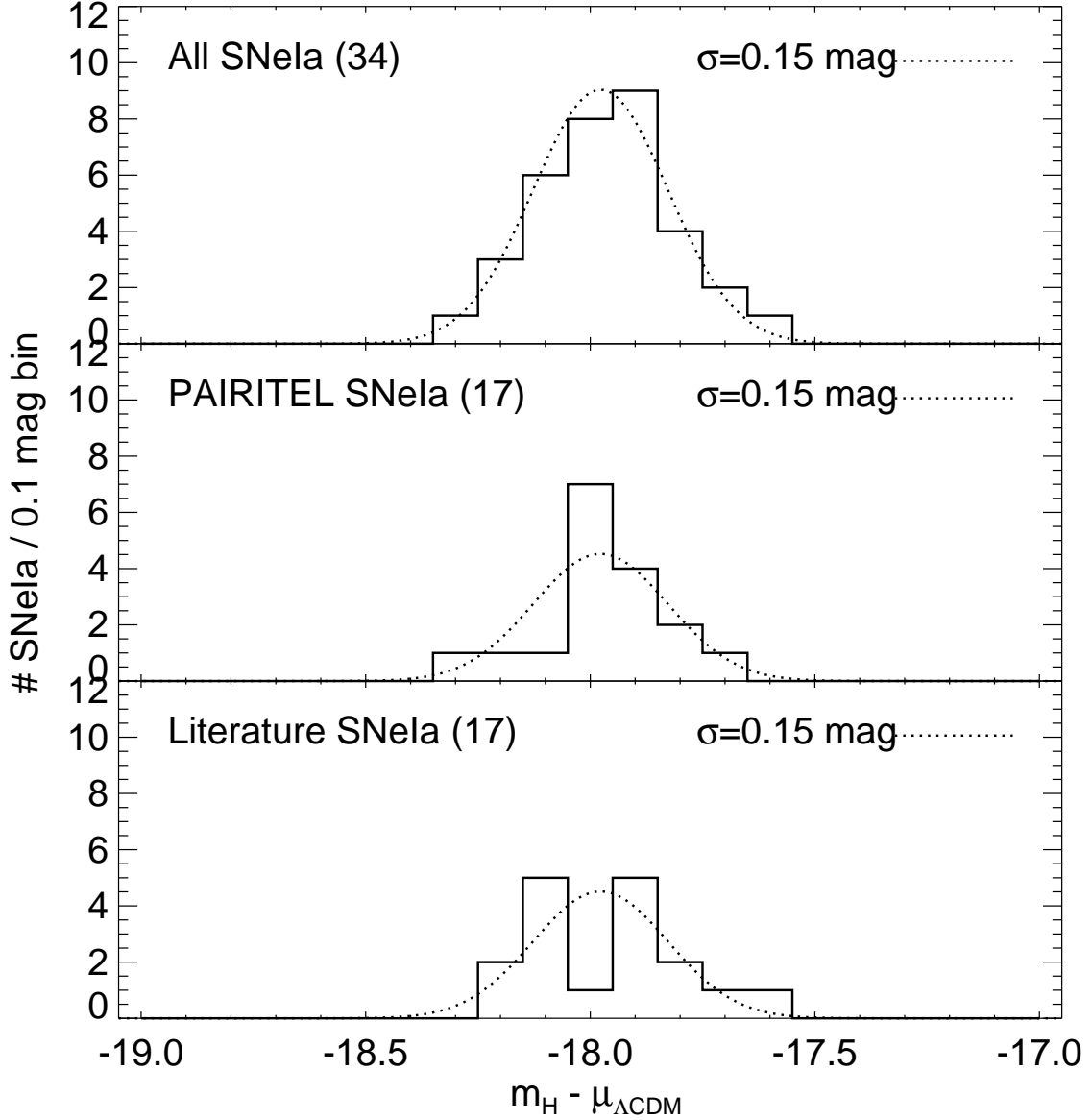


Fig. 6.— A histogram of the derived absolute magnitudes  $M_{H_{\text{Bmax}}}$  based on a  $\Lambda\text{CDM}$  cosmology with  $H_o = 72 \text{ km s}^{-1} \text{ Mpc}^{-1}$  for all SNe Ia (top panel) along with histograms for the PAIRITEL sample (middle panel) and the literature SNe Ia (bottom panel). Overlaid with each histogram is a Gaussian of width  $\sigma = 0.15 \text{ mag}$  (dotted line) normalized to the number of SNe Ia in each plot.

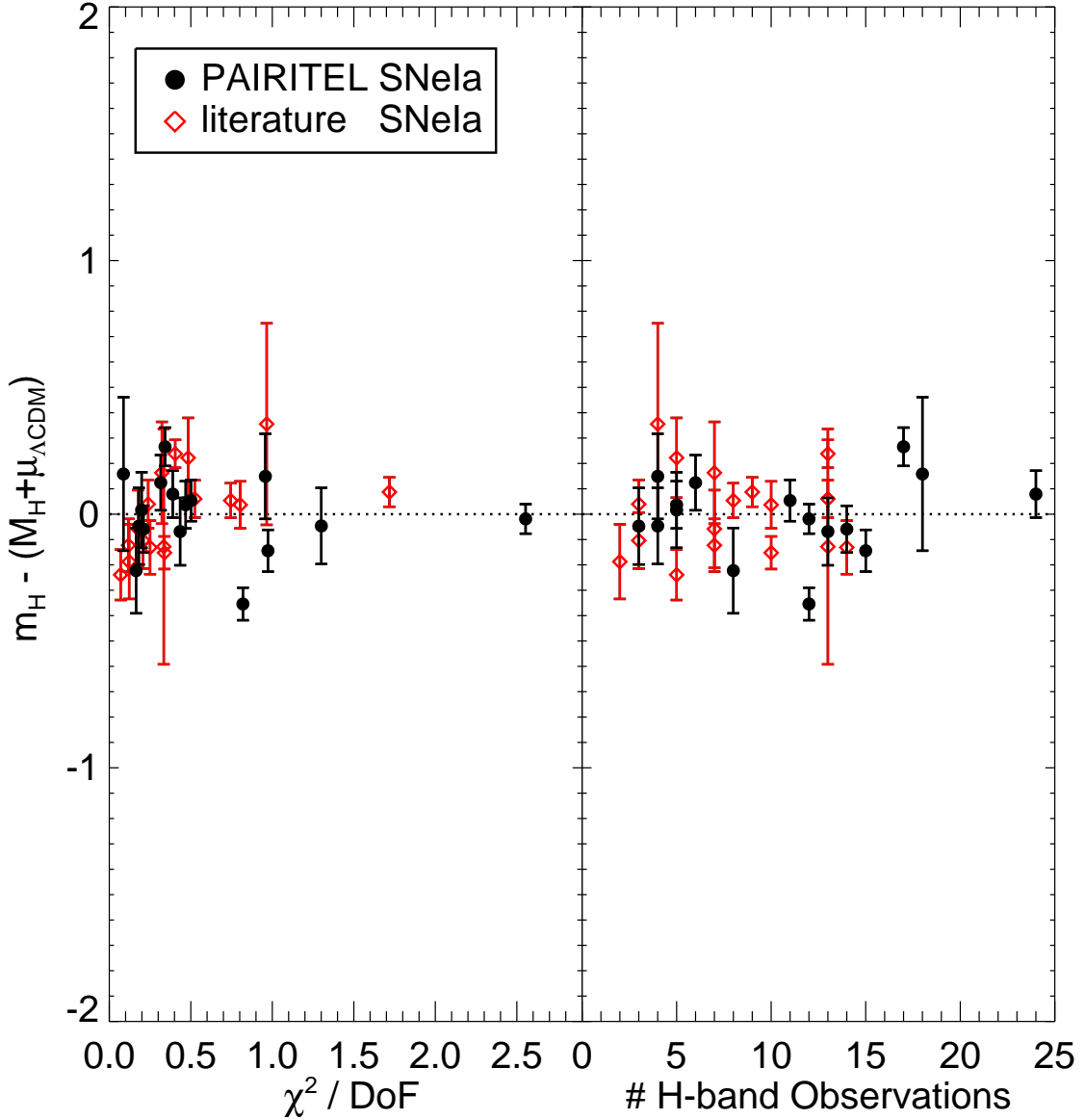


Fig. 7.— The Hubble diagram residuals as a function of  $\chi^2/\text{DoF}$  (left panel) and the number of H-band light-curve points (right panel;  $\text{DoF} = \# \text{ light-curve points} - 1$ ). These plots demonstrate that the residuals are not sensitive to the formal  $\chi^2/\text{DoF}$  of the fit and are reliable even with just a few data points. The large number of points with  $\chi^2/\text{DoF} < 1$  implies that we have likely overestimated the uncertainties in our fiducial template or in our photometric observations. Unlike in Fig. 5, the error bars show here represent both the model uncertainties (Table 2; column 7) and the peculiar velocity ( $150 \text{ km s}^{-1}$ ) (Table 2; column 4) added in quadrature (Table 2, column 12) to better allow for a relative comparison of the deviation.

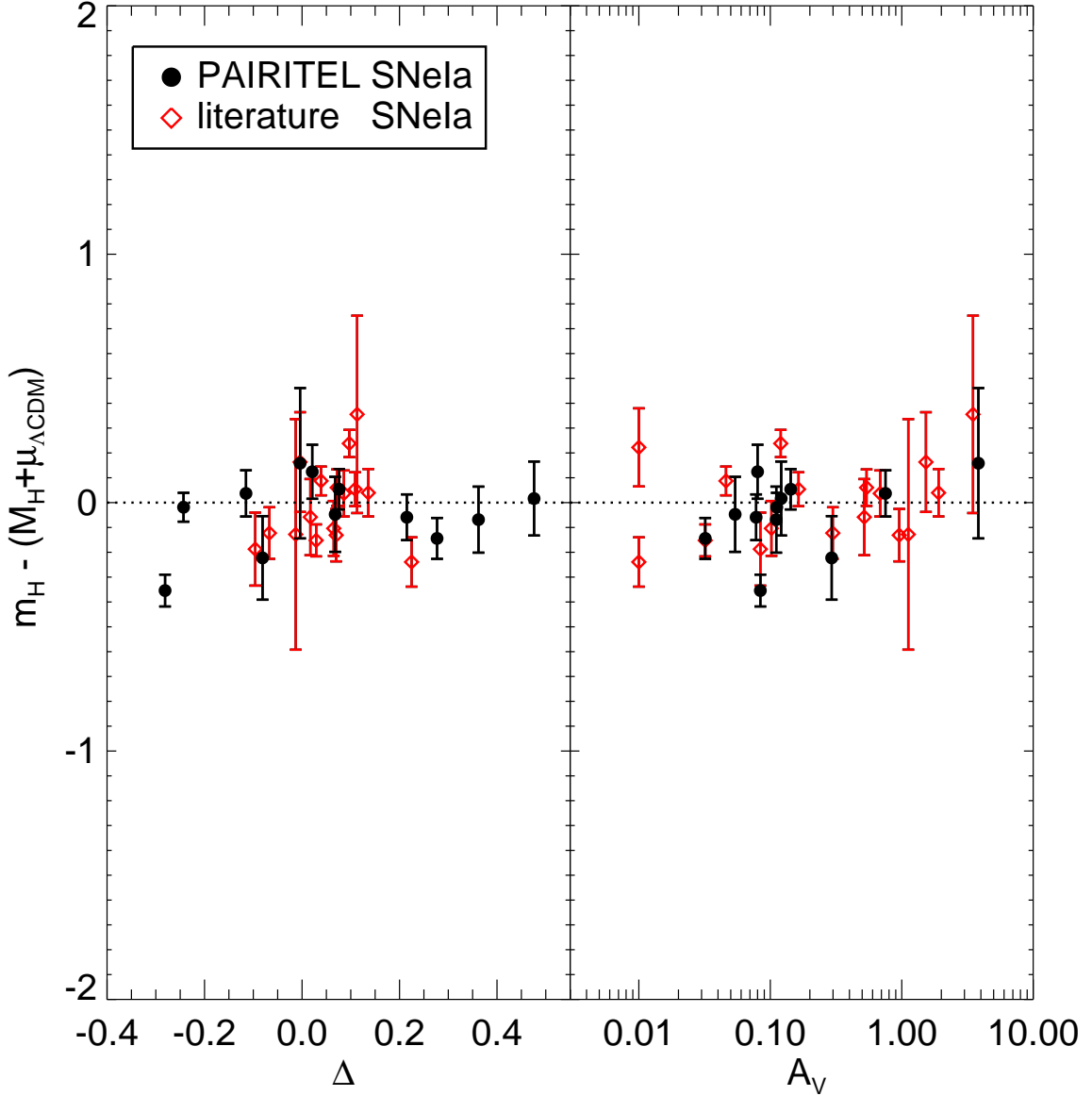


Fig. 8.— The Hubble diagram residuals as a function of the light-curve shape parameter,  $\Delta$ , and the measured optical extinction,  $A_V$ . Plotted error bars are as for Fig. 7. Both distributions are entirely consistent with no dependence of Hubble diagram residual on either optical light-curve shape or extinction. There is a mild correlation between the size of the error bars and the  $A_V$  because the SN Ia with large  $A_V$  SN Ia also tend to be nearby ( $z < 2000 \text{ km s}^{-1}$ ) due to selection effects against finding highly-extinguished supernovae at larger distances.

Table 1. SNe Ia  $JHK_s$  Peak Magnitudes

SN	$J_{\text{peak}}^{\text{b}}$	$H_{\text{peak}}^{\text{b}}$	$K_{\text{peak}}^{\text{b}}$	$N_J, N_H, N_K^{\text{a}}$	Reference <sup>c</sup>
SN 1998bu	11.55 (0.03)	11.59 (0.03)	11.42 (0.03)	18, 20, 20	J99
SN 1999cl	12.80 (0.02)	12.77 (0.04)	12.58 (0.02)	6, 5, 6	K00
SN 1999cp	14.50 (0.02)	14.77 (0.02)	14.57 (0.06)	2, 2, 2	K00
SN 1999ee	14.77 (0.03)	15.00 (0.03)	...	33, 33, 0	K04a
SN 1999ek	16.10 (0.05)	16.08 (0.04)	16.54 (0.08)	14, 15, 1	K04b
SN 1999gp	17.31 (0.06)	17.16 (0.11)	16.51 (0.15)	3, 3, 3	K01
SN 2000bh	...	16.75 (0.03)	16.64 (0.14)	0, 21, 11	K04a
SN 2000bk	17.64 (0.02)	17.45 (0.05)	...	18, 16, 0	K01
SN 2000ca	...	16.71 (0.09)	...	0, 11, 0	K04a
SN 2000ce	16.82 (0.03)	16.12 (0.03)	15.98 (0.05)	3, 5, 5	K01
SN 2001ba	...	17.24 (0.04)	17.06 (0.06)	0, 14, 9	K04a
SN 2001bt	15.34 (0.07)	15.65 (0.02)	15.40 (0.03)	21, 19, 11	K04b
SN 2001cn	15.90 (0.03)	15.66 (0.05)	15.67 (0.10)	19, 19, 3	K04b
SN 2001cz	15.40 (0.06)	15.65 (0.16)	15.40 (0.13)	12, 12, 9	K04b
SN 2002bo	13.68 (0.02)	13.82 (0.02)	13.88 (0.04)	14, 14, 14	K04b
SN 2003du	14.42 (0.02)	14.66 (0.02)	14.38 (0.02)	6, 6, 6	St07
SN 2005ao	17.90 (0.10)	17.60 (0.10)	16.8 (0.25)	6, 6, 5	WV07
SN 2005cf	13.83 (0.04)	13.96 (0.02)	13.97 (0.02)	17, 17, 15	WV07
SN 2005el	15.45 (0.02)	15.55 (0.03)	15.31 (0.03)	29, 29, 29	WV07
SN 2005eq	16.74 (0.03)	17.05 (0.08)	16.51 (0.11)	30, 26, 27	WV07
SN 2005eu	17.03 (0.09)	17.20 (0.16)	16.64 (0.22)	22, 22, 18	WV07
SN 2005hk <sup>d</sup>	15.81 (0.03)	15.60 (0.05)	15.48 (0.05)	18, 12, 13	Ph07, WV07
SN 2005iq	17.30 (0.09)	17.61 (0.19)	...	10, 3, 0	WV07
SN 2005ke <sup>d</sup>	14.18 (0.04)	13.98 (0.03)	14.03 (0.02)	19, 18, 10	WV07
SN 2005na	17.04 (0.05)	16.96 (0.14)	16.76 (0.27)	24, 19, 7	WV07
SN 2006D	14.32 (0.02)	14.47 (0.03)	14.54 (0.05)	22, 22, 20	WV07
SN 2006N	16.16 (0.11)	15.90 (0.26)	15.72 (0.32)	14, 12, 11	WV07
SN 2006X	12.86 (0.03)	12.92 (0.02)	12.74 (0.04)	60, 66, 47	WV07
SN 2006ac	16.62 (0.14)	16.60 (0.20)	16.44 (0.18)	20, 22, 15	WV07
SN 2006ax	15.81 (0.04)	16.03 (0.05)	15.94 (0.05)	18, 18, 17	WV07
SN 2006cp	17.02 (0.04)	16.96 (0.15)	16.84 (0.13)	5, 5, 3	WV07
SN 2006gr	17.9 (0.10)	17.8 (0.10)	17.7 (0.20)	6, 4, 1	WV07
SN 2006le	16.20 (0.05)	16.40 (0.10)	16.00 (0.10)	38, 32, 36	WV07
SN 2006lf	17.02 (0.04)	16.96 (0.15)	16.84 (0.13)	30, 33, 26	WV07
SN 2007cq	16.37 (0.05)	17.22 (0.10)	...	4, 2, 1	WV07

<sup>a</sup>Number of epochs w/ SNR > 3 in the  $JHK_s$  light curves, respectively.

<sup>b</sup>Magnitudes of the maximum observed magnitude in  $JHK_s$ . Magnitude errors are 1- $\sigma$  symmetric errors.

<sup>c</sup>Reference codes: WV07 (PAIRITEL photometry Wood-Vasey et al. 2007; Friedman et al. 2008); J99: Jha et al. (1999); H00: Hernandez et al. (2000); K00: Krisciunas et al. (2000); K04a: Krisciunas et al. (2004a); K04b: Krisciunas et al. (2004b); Ph06: Phillips et al. (2006); Ph07: Phillips et al. (2007); Pa07: Pastorello et al. (2007), St07: Stanishev et al. (2007).

<sup>d</sup>The unusual SN 2005hk and SN 2005ke were excluded from the template generation and fitting.

Table 2. Apparent Standard  $H$ -Band Magnitudes of Type Ia Supernovae

SN Name	$cz_{\text{CMB+Virgo}}^{\text{a}}$ km s $^{-1}$	$cz_{\text{err}}$ km s $^{-1}$	$\sigma_{\mu}(\text{vel})^{\text{b}}$ [mag]	$t_{B_{\text{max}}}$ [MJD]	$H_{B_{\text{max}}}$ [mag]	$\sigma(H_{B_{\text{max}}})$ [mag]	$\chi^2/\text{DoF}$ [mag]	DoF $^{\text{c}}$	$A_V$	$\mu^{\text{d}}$ [mag]	$\sigma_{\mu}^{\text{e}}$
SN 1998bu	709	20	0.920	50952.4	11.87	0.04	0.36	12	1.12	29.88	0.92
SN 1999cl	957	86	0.708	51342.2	13.00	0.06	1.05	3	3.49	31.01	0.71
SN 1999cp	2909	14	0.224	51363.2	14.88	0.09	0.12	1	0.08	32.89	0.24
SN 1999ee	3296	15	0.198	51469.3	15.22	0.04	0.25	13	0.96	33.23	0.20
SN 1999ek	5191	10	0.126	51481.8	16.41	0.04	0.50	12	0.54	34.41	0.13
SN 1999gp	8113	18	0.080	51550.1	17.23	0.10	0.19	2	0.10	35.24	0.13
SN 2000bh	6765	21	0.097	51636.0	16.99	0.05	0.79	7	0.16	35.00	0.11
SN 2000bk	7976	20	0.082	51647.0	17.54	0.04	0.44	12	0.12	35.55	0.09
SN 2000ca	6989	62	0.095	51666.2	16.85	0.04	0.34	9	0.03	34.86	0.10
SN 2000ce	5097	15	0.128	51667.3	16.35	0.07	0.27	2	1.90	34.35	0.14
SN 2001ba	8718	22	0.075	52034.2	17.59	0.04	1.77	8	0.05	35.60	0.09
SN 2001bt	4220	13	0.155	52062.9	15.92	0.05	0.80	9	0.69	33.93	0.16
SN 2001cn	4454	250	0.190	52071.0	15.95	0.05	0.19	6	0.52	33.96	0.20
SN 2001cz	4506	20	0.145	52103.4	15.91	0.07	0.12	6	0.30	33.92	0.16
SN 2002bo	1696	20	0.385	52356.0	14.06	0.05	0.33	6	1.53	32.07	0.39
SN 2003du	2206	14	0.296	52765.9	14.69	0.05	0.54	4	0.01	32.70	0.30
SN 2004eo	4859	17	0.134	53278.7	15.96	0.07	0.07	4	0.01	33.97	0.15
SN 2005ao	11828	126	0.060	53442.0	18.19	0.09	0.77	1	0.10	36.20	0.11
SN 2005cf	2018	11	0.323	53533.6	14.05	0.05	0.16	7	0.29	32.06	0.33
SN 2005el	4349	8	0.150	53646.1	15.81	0.03	0.95	14	0.03	33.82	0.15
SN 2005eq	8535	25	0.077	53653.9	17.43	0.04	2.58	11	0.11	35.43	0.09
SN 2005eu	10503	14	0.062	53659.8	17.56	0.05	0.86	11	0.08	35.57	0.08
SN 2005iq	10102	40	0.065	53687.1	17.77	0.15	0.18	2	0.05	35.78	0.16
SN 2005na	7826	26	0.084	53740.5	17.38	0.10	0.32	5	0.08	35.39	0.13
SN 2006D	2560	18	0.255	53756.7	14.73	0.03	0.43	12	0.11	32.74	0.26
SN 2006N	4468	27	0.146	53760.6	16.03	0.13	0.20	4	0.12	34.04	0.19
SN 2006X	1091	20	0.598	53785.5	13.09	0.03	0.09	17	3.83	31.10	0.60
SN 2006ac	7123	17	0.092	53781.2	16.98	0.08	0.21	13	0.08	34.99	0.12
SN 2006ax	4955	20	0.132	53826.7	16.29	0.05	0.51	10	0.14	34.30	0.14
SN 2006cp	6816	14	0.096	53896.7	16.98	0.08	0.49	4	0.75	34.99	0.12
SN 2006gr	10547	22	0.062	54014.0	18.06	0.16	0.95	3	...	36.07	0.18
SN 2006le	5403	12	0.121	54048.0	16.70	0.05	0.35	16	...	34.71	0.13
SN 2006lf	4048	10	0.161	54047.0	15.88	0.05	0.39	23	...	33.89	0.17

Table 2—Continued

SN Name	$cz_{\text{CMB+Virgo}}^{\text{a}}$ km s <sup>-1</sup>	$cz_{\text{err}}$ km s <sup>-1</sup>	$\sigma_{\mu}(\text{vel})^{\text{b}}$ [mag]	$t_{B_{\text{max}}}$ [MJD]	$H_{B_{\text{max}}}$ [mag]	$\sigma(H_{B_{\text{max}}})$ [mag]	$\chi^2/\text{DoF}$ [mag]	DoF <sup>c</sup>	$A_V$	$\mu^{\text{d}}$ [mag]	$\sigma_{\mu}^{\text{e}}$
SN 2007cq	7501	50	0.088	54272.5	17.11	0.14	1.37	3	...	35.12	0.17

<sup>a</sup>Redshift of host galaxies as corrected to CMB frame with the additional correction of Virgo member NGC 4501 (host of SN 1999cl) from its observed CMB-corrected recession velocity (2281 km/s) to the mean recession velocity of Virgo (957 km/s).

<sup>b</sup>A peculiar velocity of 150 km/s and the individual redshift measurement uncertainty of column 2 was converted into an equivalent distance modulus uncertainty using Eq. 1.

<sup>c</sup>DoF: The number of degrees of freedom is the number of  $H$ -band data points minus 1 for the overall offset fit parameter,  $H_{B_{\text{max}}}$ .

<sup>d</sup>Assuming  $H_0 = 72 \text{ km s}^{-1} \text{ Mpc}^{-1}$  and thus  $M_H = 17.96 \text{ mag}$ .

<sup>e</sup>Quadrature sum of peculiar velocity distance modulus uncertainty (column 4) and fit uncertainty (column 7).

Table 3. Light Curve Table Stub

SN	MJD	Passband	Flux <sub>25</sub> <sup>a</sup>	Flux err <sub>25</sub>
2005ao	53440.4157	H	600.2491	3.5737
2005ao	53456.4300	H	437.9836	3.6405
2005ao	53464.3872	H	339.2386	128.0434
2005ao	53466.3879	H	345.1047	90.6351
2005ao	53467.3847	H	561.7854	3.7594
...				

<sup>a</sup>Fluxes are expressed normalized to a zeropoint of 25. I.e., the calibrated 2MASS magnitude is  $\text{mag} = -2.5 \log_{10}(\text{flux}) + 25$

Note. — This is a representative stub of the light-curve table.  $JHK_s$  light curves for all 17 PAIRITEL SNe Ia presented in this paper are available in the online electronic version.